Ligand-Directed Assembly and Transformation of Hybrid Oxo-Vanadates into 3d–3d Oxo-Vanado-Cuprates: Structural Diversification and Superior Electrochemical Performance in Prototype Liquid Configured Device Grade Supercapacitor

Kalyankumar S. Morla,[a] Rajulal Sahu,[b] Subuhan Ahamed,[c] Saurav Ghosh,[c] Kartik Chandra Mondal,[c] Babasaheb R. Sankapal,[b]* Abhishek Banerjee[a]*

[a]: Department of Chemistry, Visvesvaraya National Institute of Technology, Nagpur – 440010, India.

[b]: Department of Physics, Visvesvaraya National Institute of Technology, Nagpur – 440010, India.

[c]: Department of Chemistry, Indian Institute of Technology Madras, Chennai – 600036, India.

Email: abhishekbanerjee@chm.vnit.ac.in, brsankapal@gmail.com

Supporting Information

Table S1. Bond Valence Sum (BVS) calculations of **CuV-1**

Bond	Bond Length	Bond Valence	Bond Valence Sum
V3-O22	1.5960 (0)	1.6621	∑(V3) = 4.1354
V3-O23	2.3045 (0)	0.2449	
V3-O24	1.9884 (0)	0.5755	
V3-O34	1.9996 (1)	0.5584	
V3-O6	1.9773 (1)	0.5931	
V3-O1	2.0395 (1)	0.5013	

Bond	Bond Length	Bond Valence	Bond Valence Sum
V1-O20	1.6246 (1)	1.6196	∑(V1) = 4.9760
V1-O21	1.6303 (0)	1.5948	
V1-O7	2.01 (1)	0.5715	
V1-O4	2.0205 (0)	0.5555	
V1-O30	1.9713 (1)	0.6345	

Bond	Bond Length	Bond Valence	Bond Valence Sum
V2-O10	2.0289 (1)	0.5430	∑(V2) = 5.0975
V2-O3	1.9451 (1)	0.6811	
V2-O33	1.6352 (0)	1.5738	
V2-O32	1.6249 (1)	1.6182	
V2-O9	1.9476 (1)	0.6765	

Bond	Bond Length	Bond Valence	Bond Valence Sum
Cu1-N1	1.9786 (1)	0.4449	∑(Cu1) = 2.4118
Cu1-N2	1.9828 (1)	0.4399	
Cu1-O4	1.9425 (1)	0.4906	
Cu1-O7	2.721 (1)	0.0598	
Cu1-O3	2.6887 (1)	0.0793	
Cu1-O10	1.9236 (1)	0.6272	

Table S2. Bond Valence Sum (BVS) calculations polyanion **CuV-2**

Bond	**Bond Length**	**Bond Valence**	**Bond Valence Sum**
V1-O1	1.6444 (0)	1.4583	∑(V1) = 4.1877
V1-O2	2.3315 (1)	0.2277	
V1-O3	1.9517 (1)	0.6355	
V1-O4	1.9637 (1)	0.6153	
V1-O3	1.9517 (1)	0.6355	
V1-O4	1.9637 (1)	0.6153	

Bond	**Bond Length**	**Bond Valence**	**Bond Valence Sum**
V2-O1	1.6068 (0)	1.6994	∑(V2) = 5.1321
V2-O11	1.6308 (0)	1.5927	
V2-O12	1.997 (0)	0.5919	
V2-O9	2.0077 (0)	0.5751	
V2-O7	1.9495 (0)	0.6730	

Bond	**Bond Length**	**Bond Valence**	**Bond Valence Sum**
V3-O14	1.611 (0)	1.6802	∑(V3) = 5.2282
V3-O12	1.9898 (0)	0.6035	
V3-O13	1.6016 (0)	1.7234	
V3-O8	1.9686 (0)	0.6392	
V3-O9	2.0034 (0)	0.5818	

Bond	Bond Length	Bond Valence	Bond Valence Sum
Cu1-N1	1.9824 (0)	0.4404	∑(Cu1) = 2.0455
Cu1-N1	1.9824 (0)	0.4404	
Cu1-O16	2.4125 (1)	0.1377	
Cu1-O15	2.0292 (0)	0.3881	
Cu1-O16	2.4125 (1)	0.1673	
Cu1-O15	2.0292 (0)	0.4715	

Table S3: Hydrogen-bonding parameters for compound CuV-1

Donor - H ⋯ Acceptor	D – H (Å)	H ⋯ A (Å)	D ⋯ A (Å)
O1V3 – H13A···O1P2$^{\#1}$	0.84	2.58	2.977
O1V3 – H13B···O1P2$^{\#1}$	0.84	2.20	2.977
C9 – H9A···O1P1$^{\#2}$	0.97	2.54	3.030
C9 – H9A···O3P4	0.97	2.56	3.474
C14 – H14···O5W$^{\#3}$	0.93	2.45	3.293
O1V3 – H13A···O2P3	0.58	2.58	3.342
O1V3 – H13A···O2V1	0.58	2.30	2.846

Symmetry transformations used to generate equivalent atoms:

$^{\#1}$: $^{1}/_{2}$ - x, $^{1}/_{2}$ - y, 1-z

$^{\#2}$: - x, 1- y, -½ + z

$^{\#3}$: - x, 1- y, ½ - z

Table S4: Hydrogen-bonding parameters for compound CuV-2

Donor - H ⋯ Acceptor	D – H (Å)	H ⋯ A (Å)	D ⋯ A (Å)
C4 – H6···O10$^{\#1}$	0.93	2.53	3.439
C9 – H9B···O10$^{\#2}$	0.96	2.43	3.323
C4 – H4···O6	0.93	2.46	3.144

Symmetry transformations used to generate equivalent atoms:

$^{\#1}$: $^{3}/_{2}$ - x, - y, z

$^{\#2}$: $^{3}/_{2}$ - x, - y, 1+z

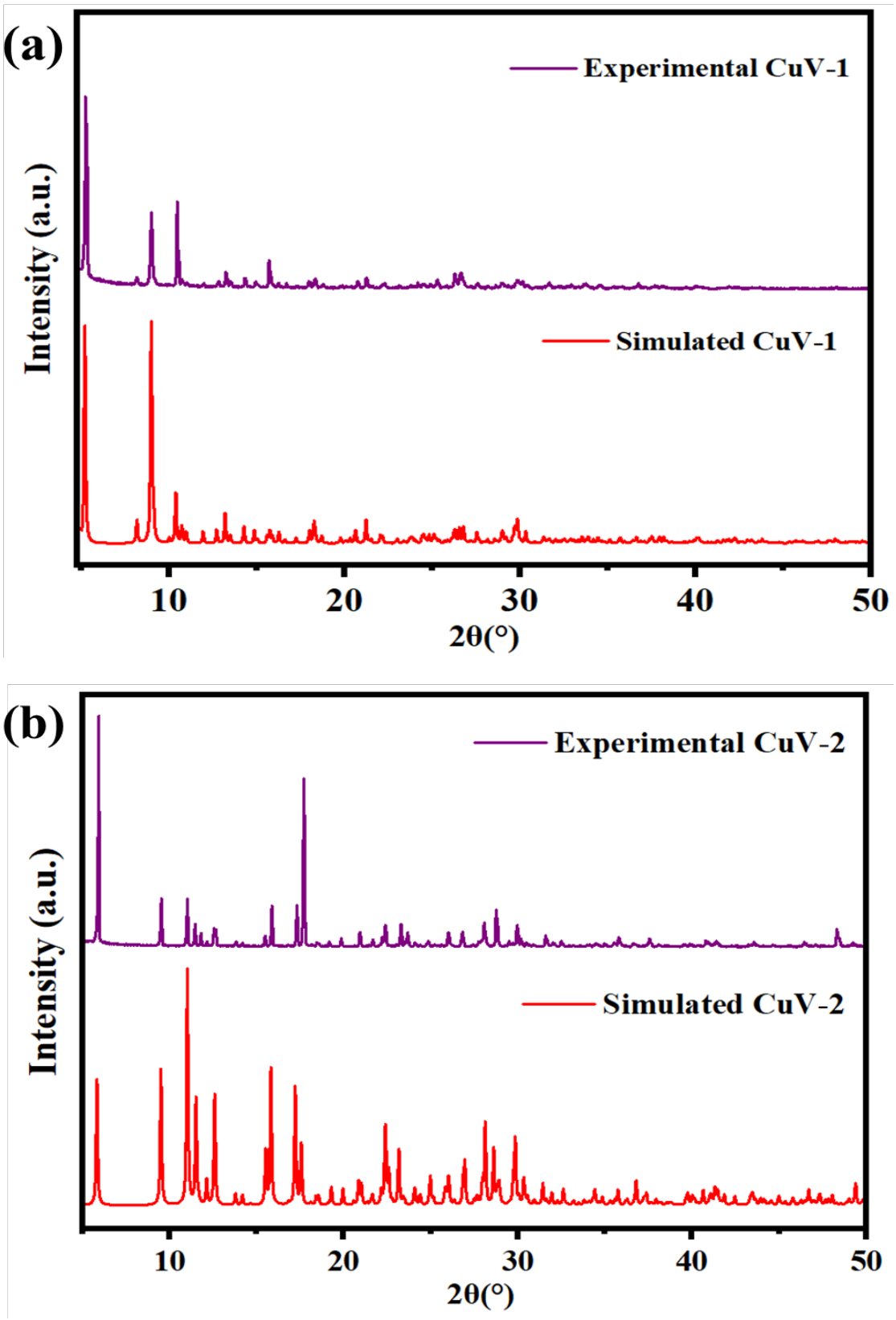

Figure S1. Comparative powder XRD pattern of **(a)** compound **CuV-1a** and **(b)** compound **CuV-2a** (Simulated vs. Experimental).

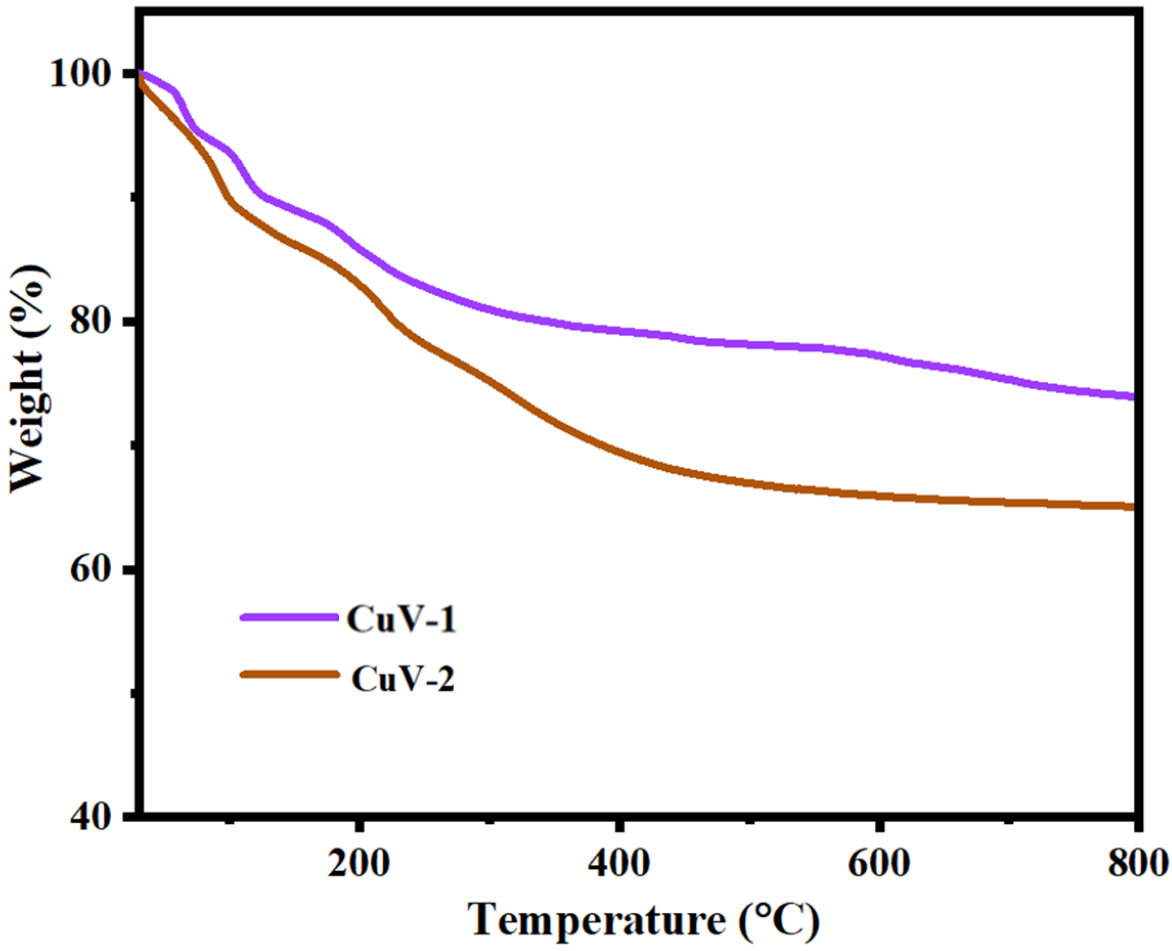

Figure S2: TGA Plots for compounds **CuV-1a** and **CuV-2a**.

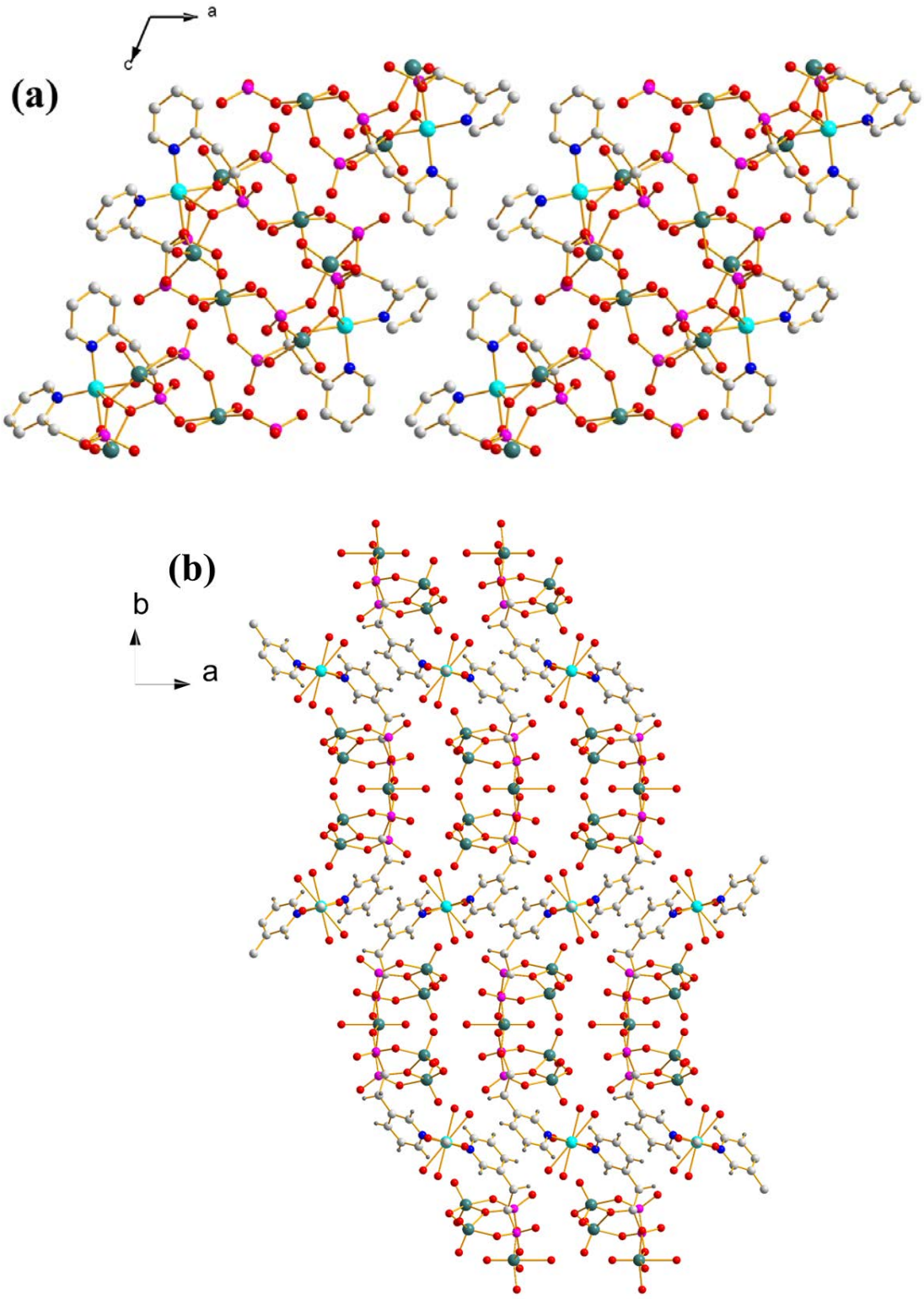

Figure S3. Crystal packing arrangement for polyanions **CuV-1** and **CuV-2**, **(a)** along the b-axis, **(b)** along the c-axis.

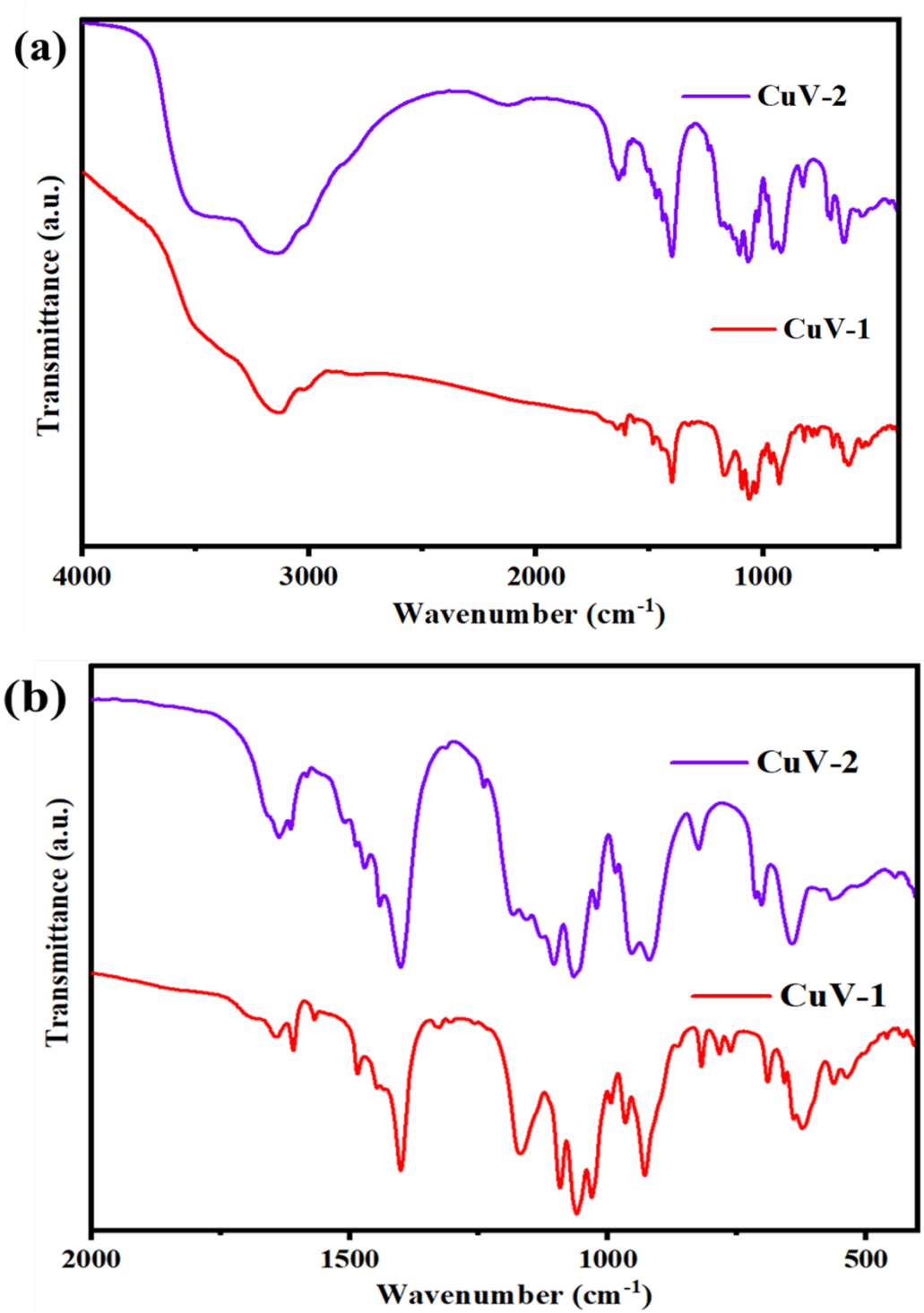

Figure S4. Comparative infrared spectra of compounds **CuV-1a** and **CuV-2a**, **(a)** Complete spectra, **(b)** fingerprint region.

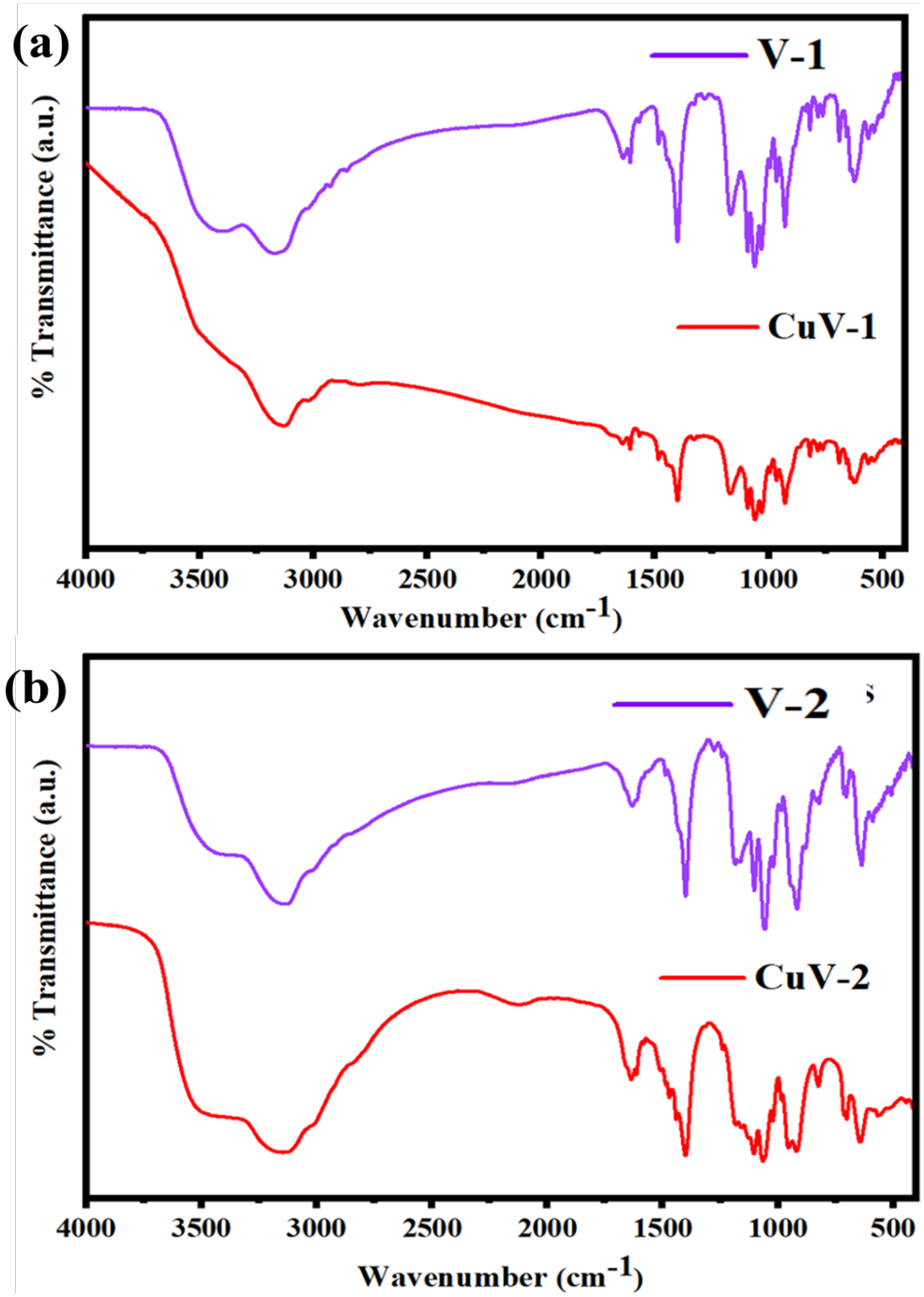

Figure S5. Comparative IR spectra of **(a)** compound **CuV-1a** vs **V-1 (b)** compound **CuV-2a** vs **V-2.**

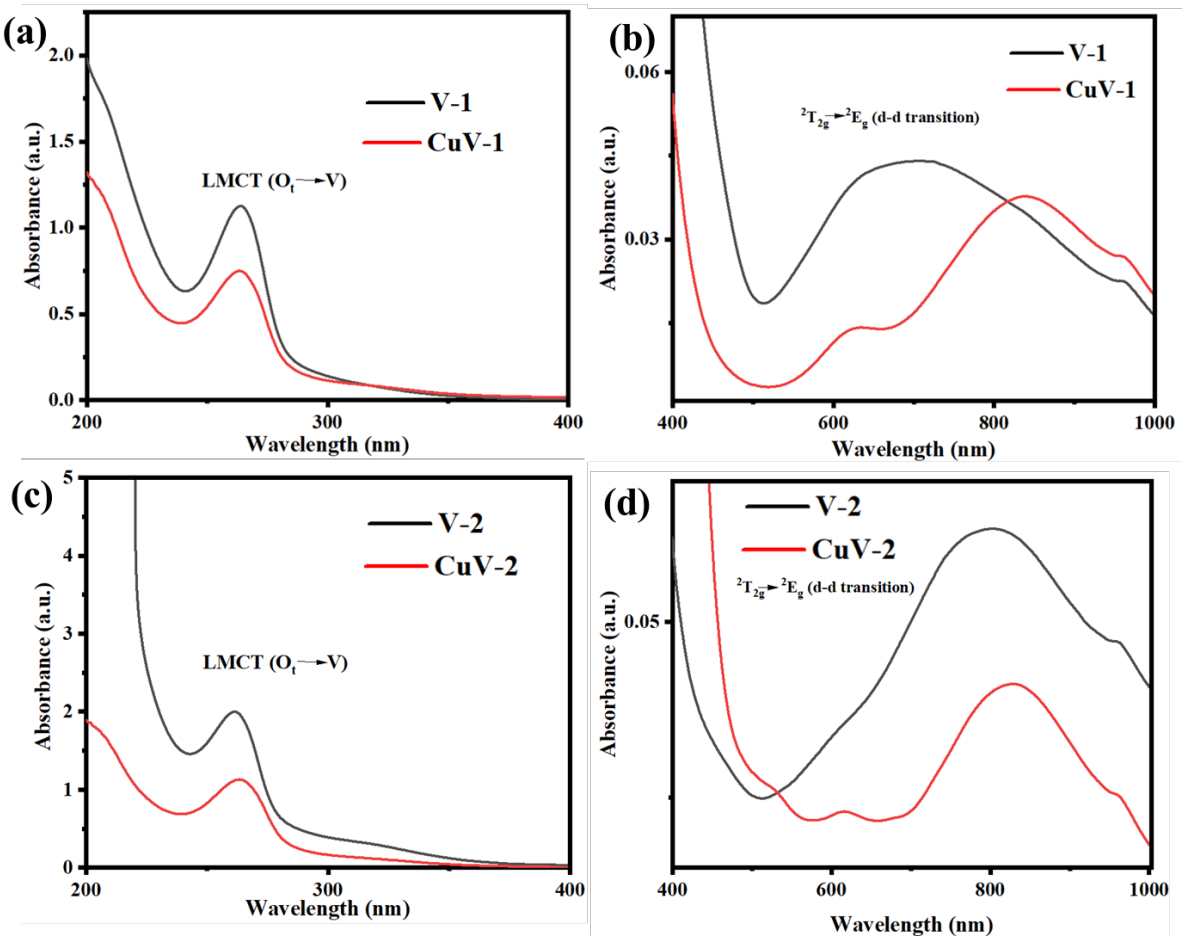

Figure S6. Comparative UV-vis spectra **(a) V-1** *vs* **CuV-1** (200-400 nm), **(b) V-1** *vs* **CuV-1** (400-1000 nm), **(c) V-2** *vs* **CuV-2** (200-400 nm), and **(d) V-2** *vs* **CuV-2** (400-1000 nm).

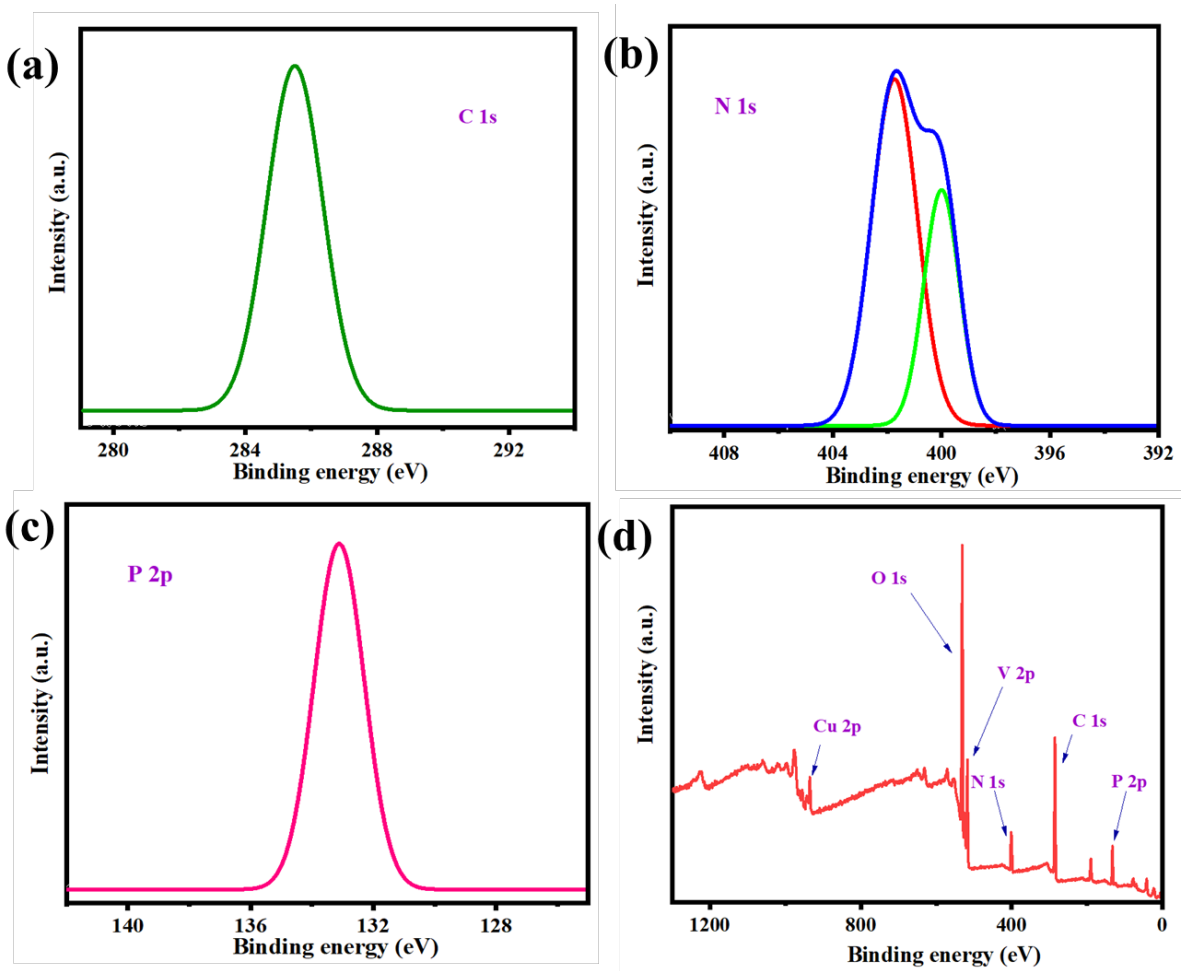

Figure S7. XPS Spectra of compound **CuV-1a**, **(a)** C 1s, **(b)** N 1s, **(c)** P 2p, and, **(d)** Survey spectrum.

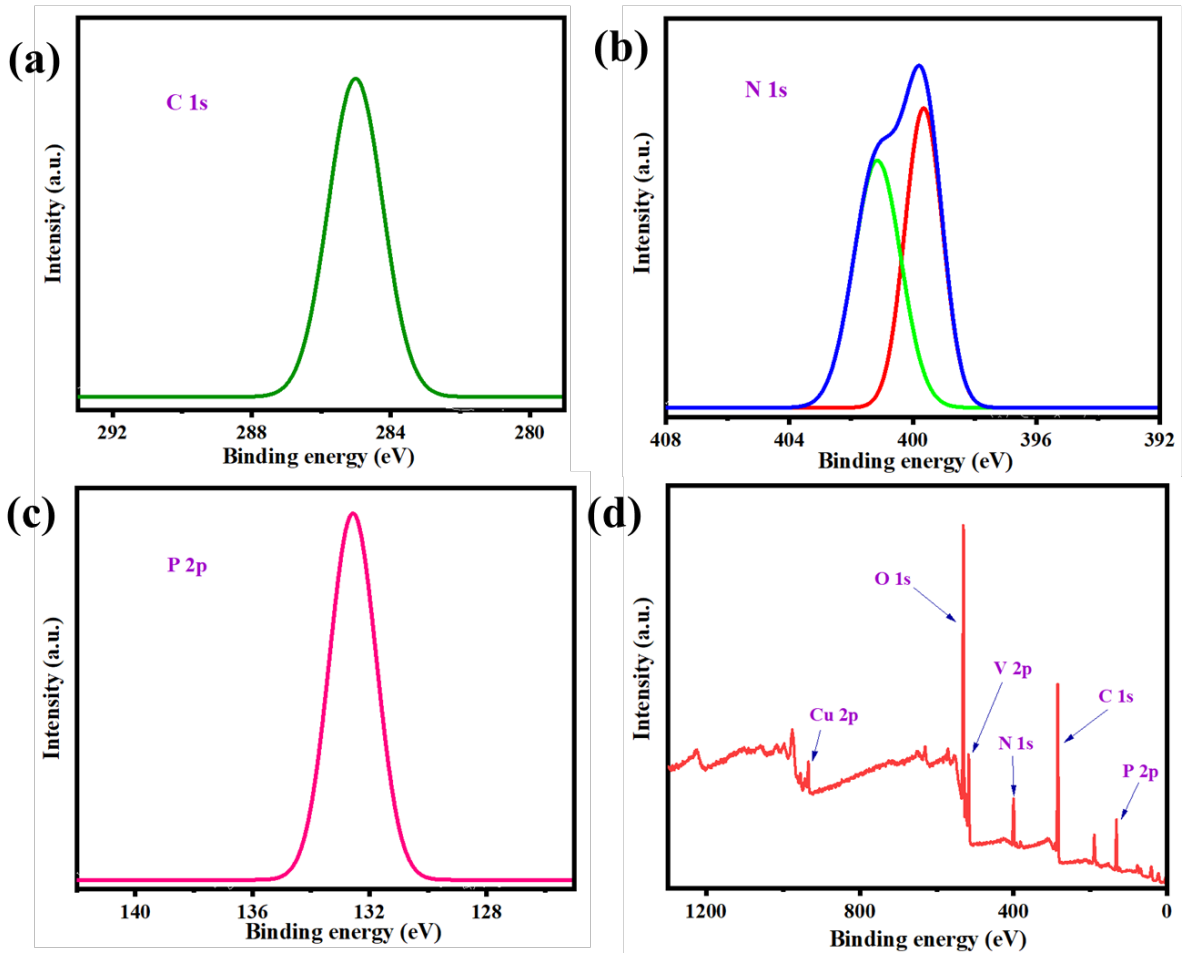

Figure S8. XPS Spectra of compound **CuV-2a**, **(a)** C 1s, **(b)** N 1s, **(c)** P 2p, and, **(d)** Survey spectrum.

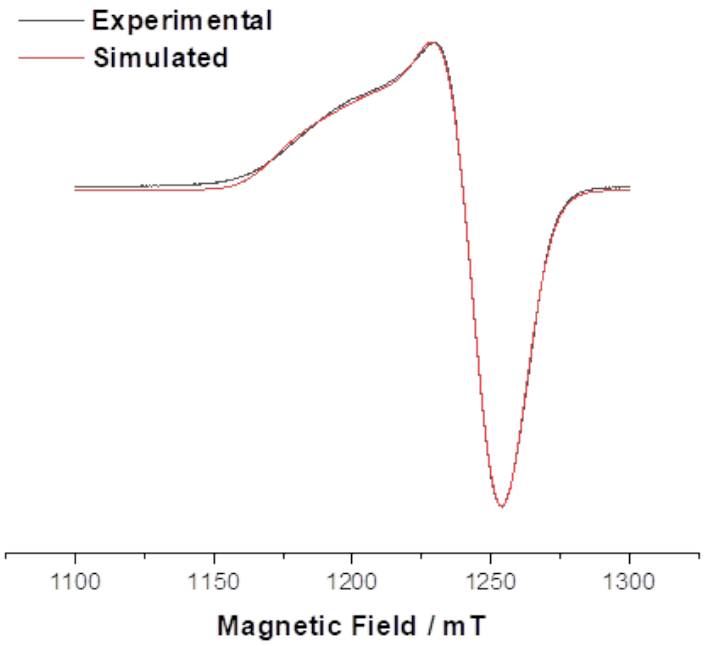

(a)

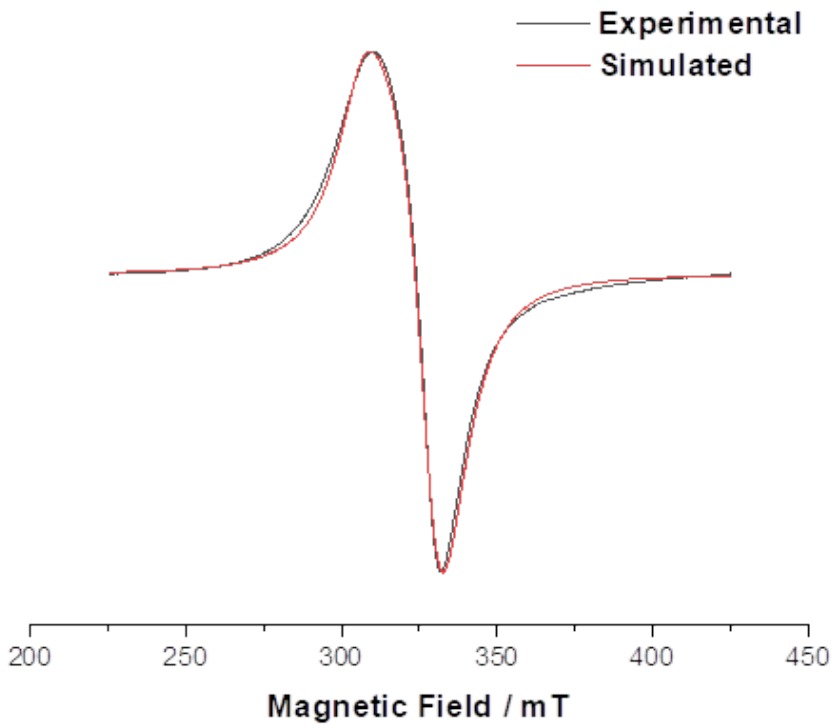

(b)

Figure S9: **(a)** Q-Band EPR spectrum of complex **CuV-1**. **(b)** X-Band EPR spectrum of complex **CuV-2**. Red and black lines represent the simulated and the experimental spectra of the complex, and the simulation is done using the EasySpin program.[S11]

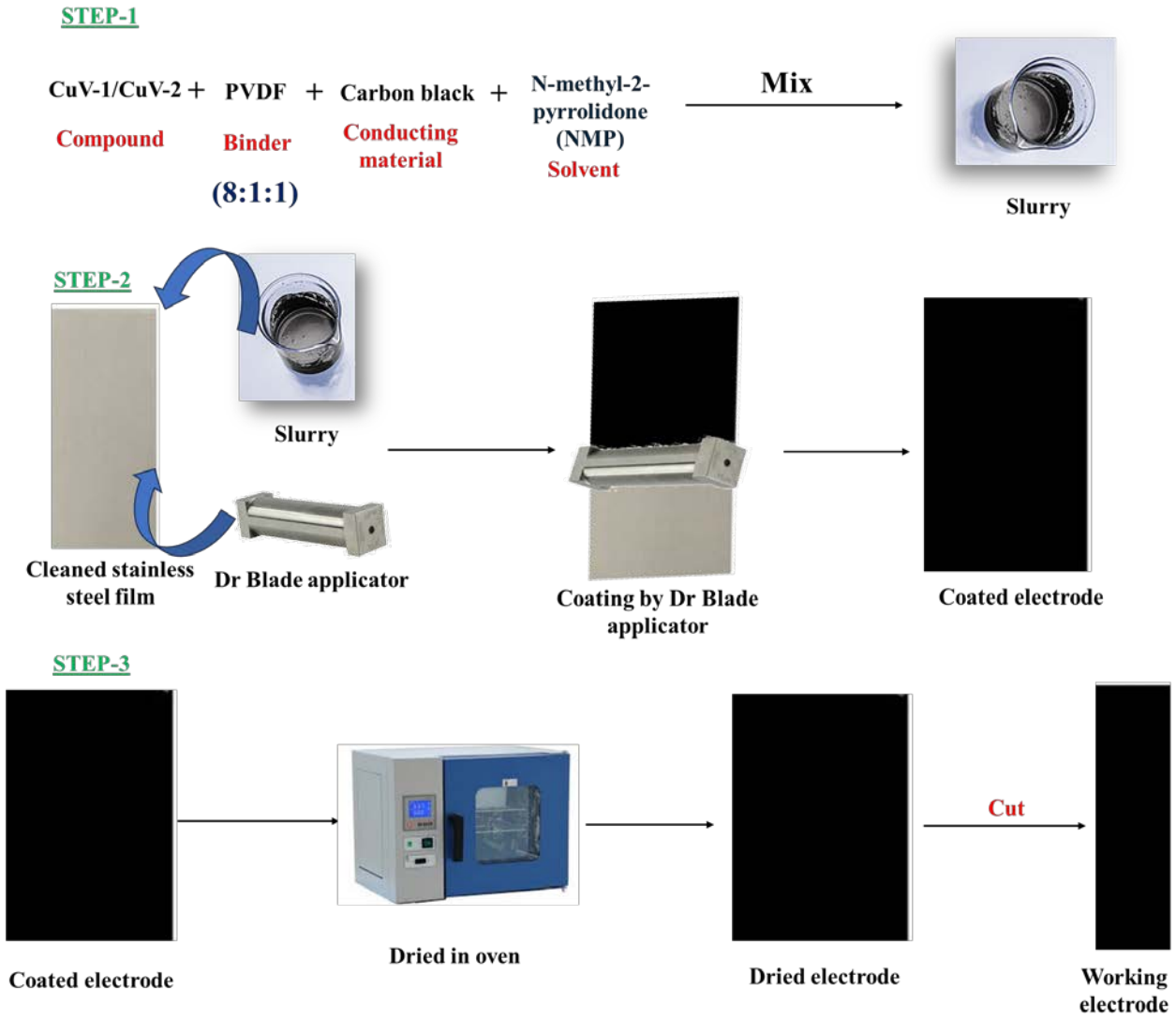

Figure S10. Scheme for the preparation of electrodes **CuV-SS-1** and **CuV-SS-2** using Dr blade method.

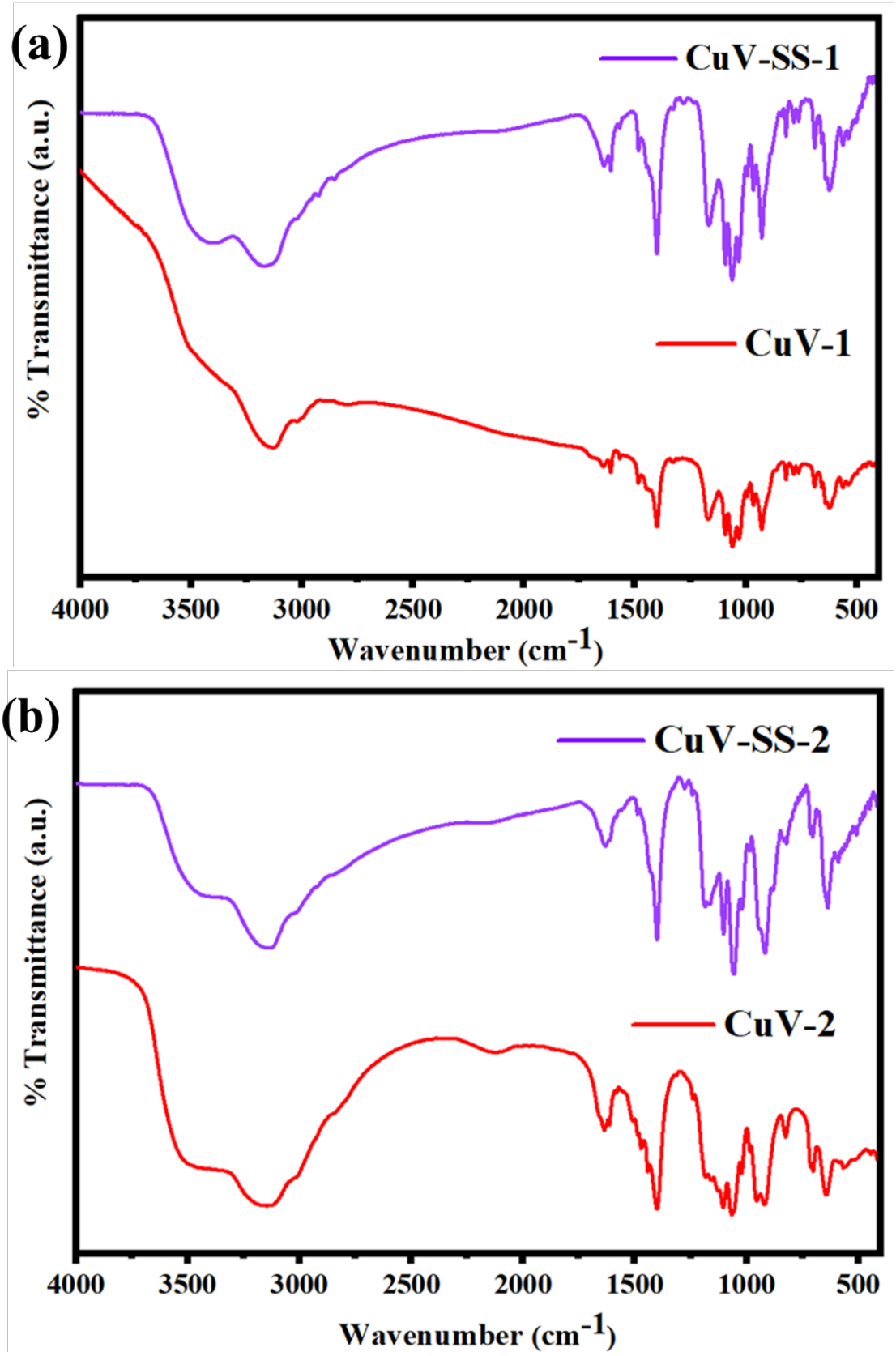

Figure S11. Comparative IR spectra of **(a)** compound **CuV-1a** vs electrode **CuV-SS-1**, **(b)** compound **CuV-2a** vs electrode **CuV-SS-2.**

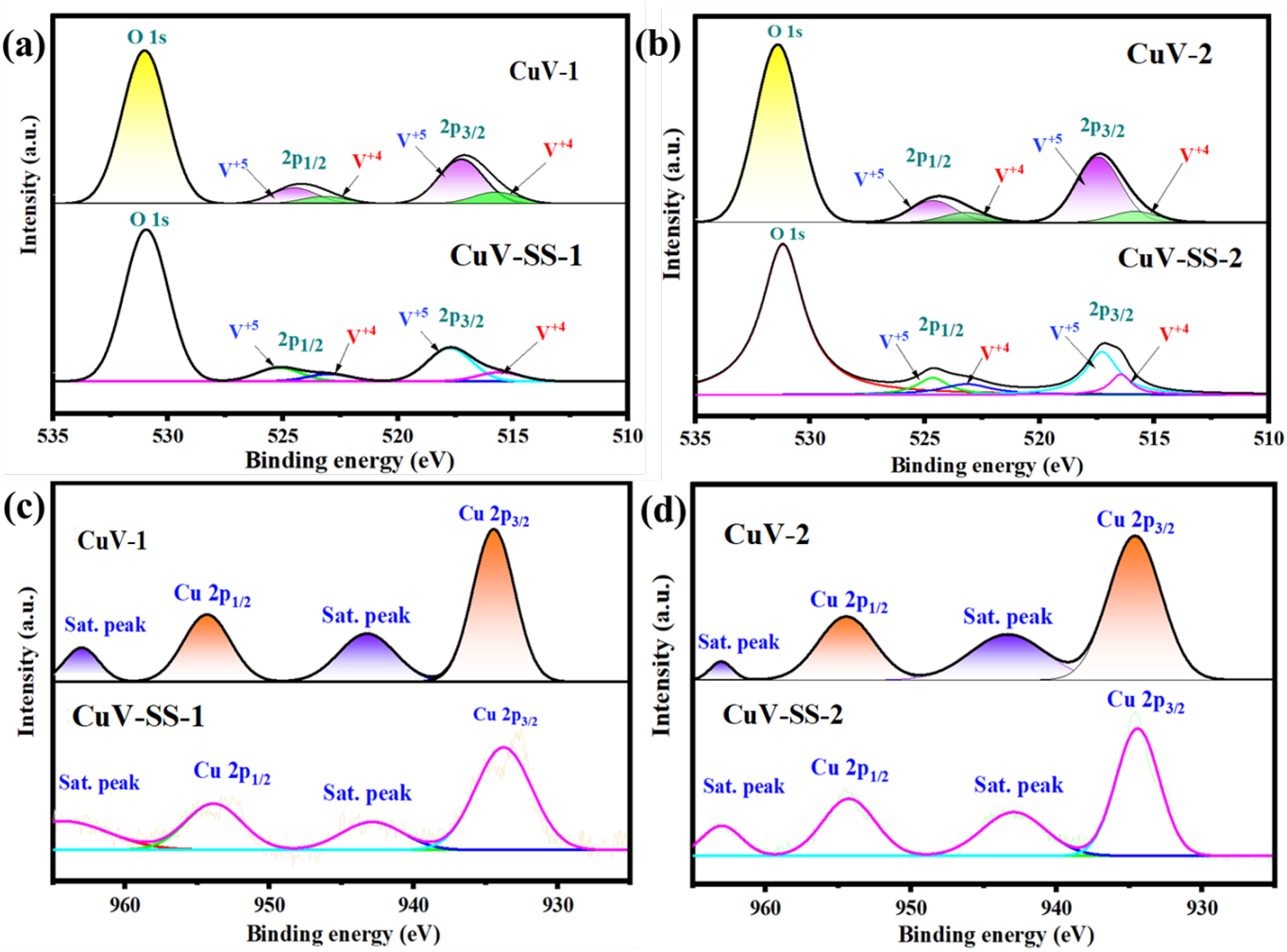

Figure S12. XPS spectra of electrodes, **(a)** V $2p_{1/2}$ and V $2p_{3/2}$ of **CuV-1** *vs* **CuV-SS-1**, **(b)** V $2p_{1/2}$ and V $2p_{3/2}$ of **CuV-2** vs **CuV-SS-2** (**c)** Cu $2p_{1/2}$ and Cu $2p_{3/2}$ of **CuV-1** vs **CuV-SS-1**, **(d)** Cu $2p_{1/2}$ and Cu $2p_{3/2}$ of **CuV-2** vs **CuV-SS-2**.

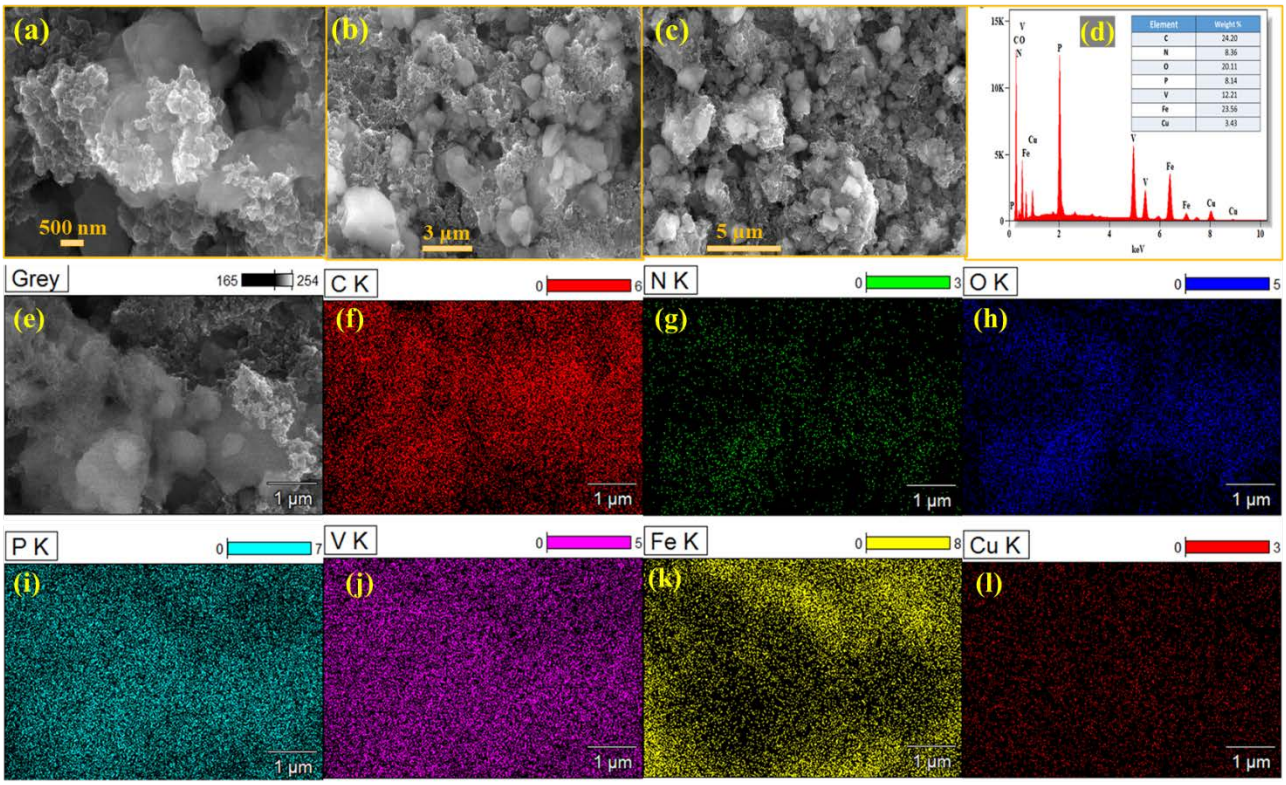

Figure S13. SEM images for **CuV-SS-1 (a)** at 500 nm scale **(b)** at 3 µm scale, **(c)** at 5 µm scale, **(d)** EDX spectra of **CuV-SS-1** (Inset shows tabular form of elemental composition), **(e-f)** Elemental mapping for **CuV-SS-1** with respective elements at 1 µm scale.

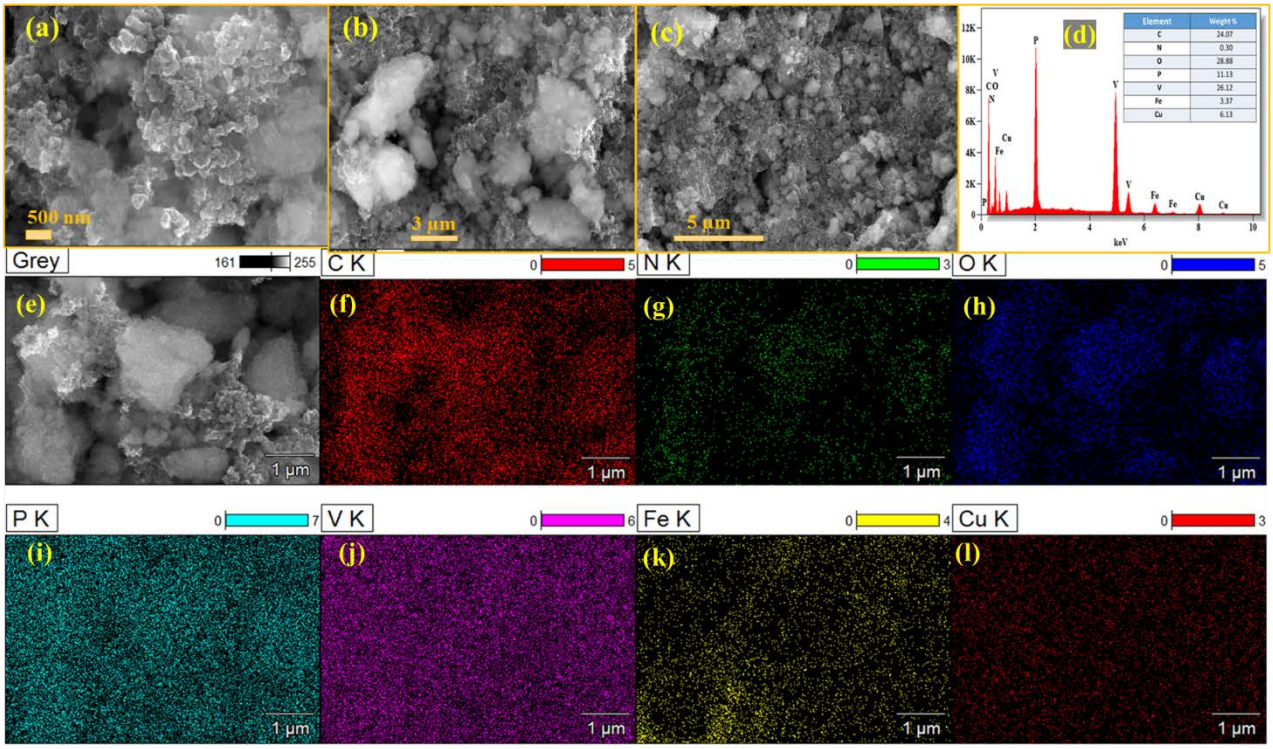

Figure S14. SEM images for **CuV-SS-2 (a)** at 500 nm scale **(b)** at 3 µm scale, **(c)** at 5 µm scale, **(d)** EDX spectra of **CuV-SS-2** (Inset shows tabular form of elemental composition), **(e-f)** Elemental mapping for **CuV-SS-2** with respective elements at 1 µm scale.

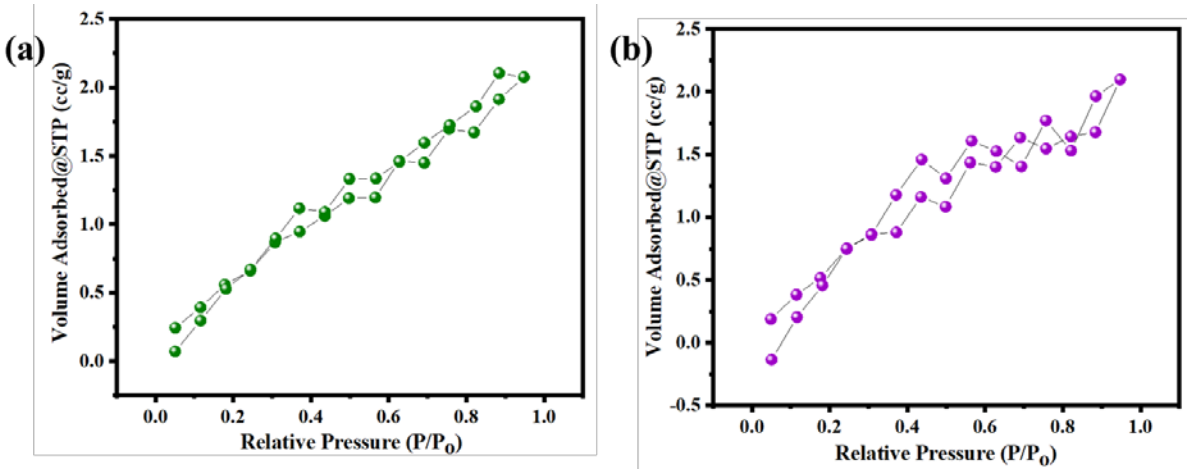

Figure S15. BET isotherms for electrode materials **(a) CuV-SS-1** and **(b) CuV-SS-2**.

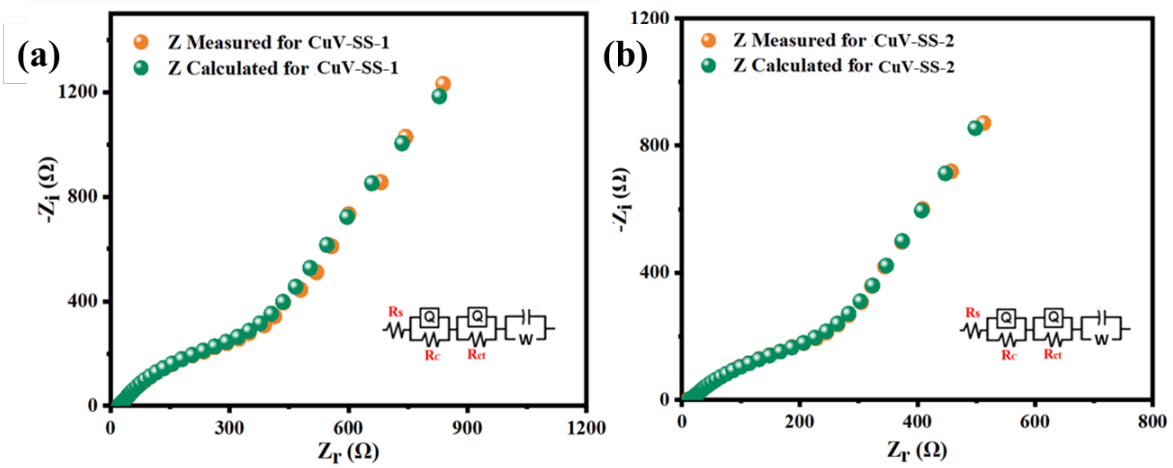

Figure S16. Electrochemical impedance spectroscopy (EIS) analysis: Nyquist plots of electrodes **(a) CuV-SS-1** and **(b) CuV-SS-2.** (inset shows fitting circuit)

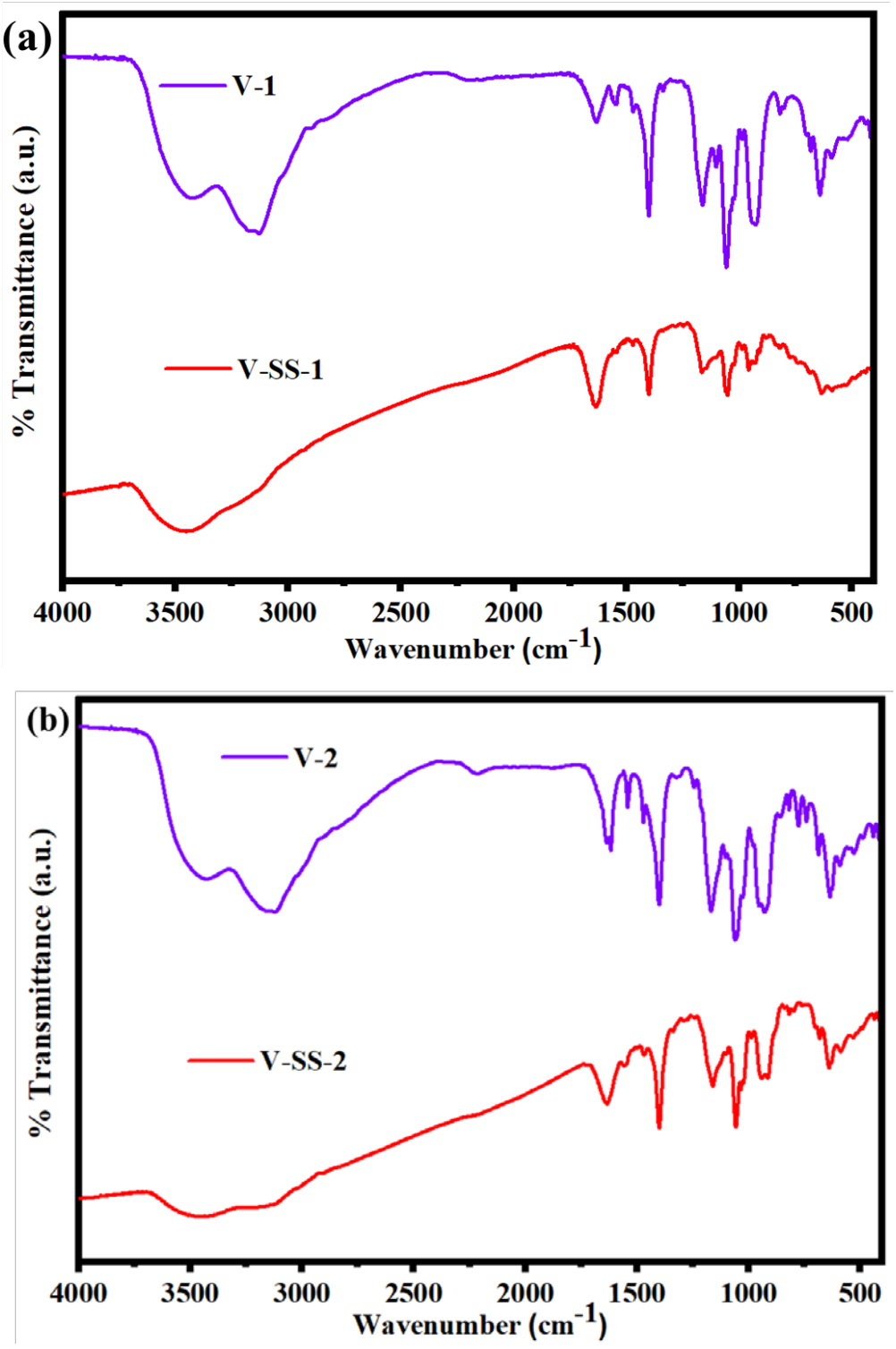

Figure S17. Comparative IR spectra of **(a)** compound **V-1a** vs electrode **V-SS-1**, **(b)** compound **2a** vs electrode **V-SS-2.**

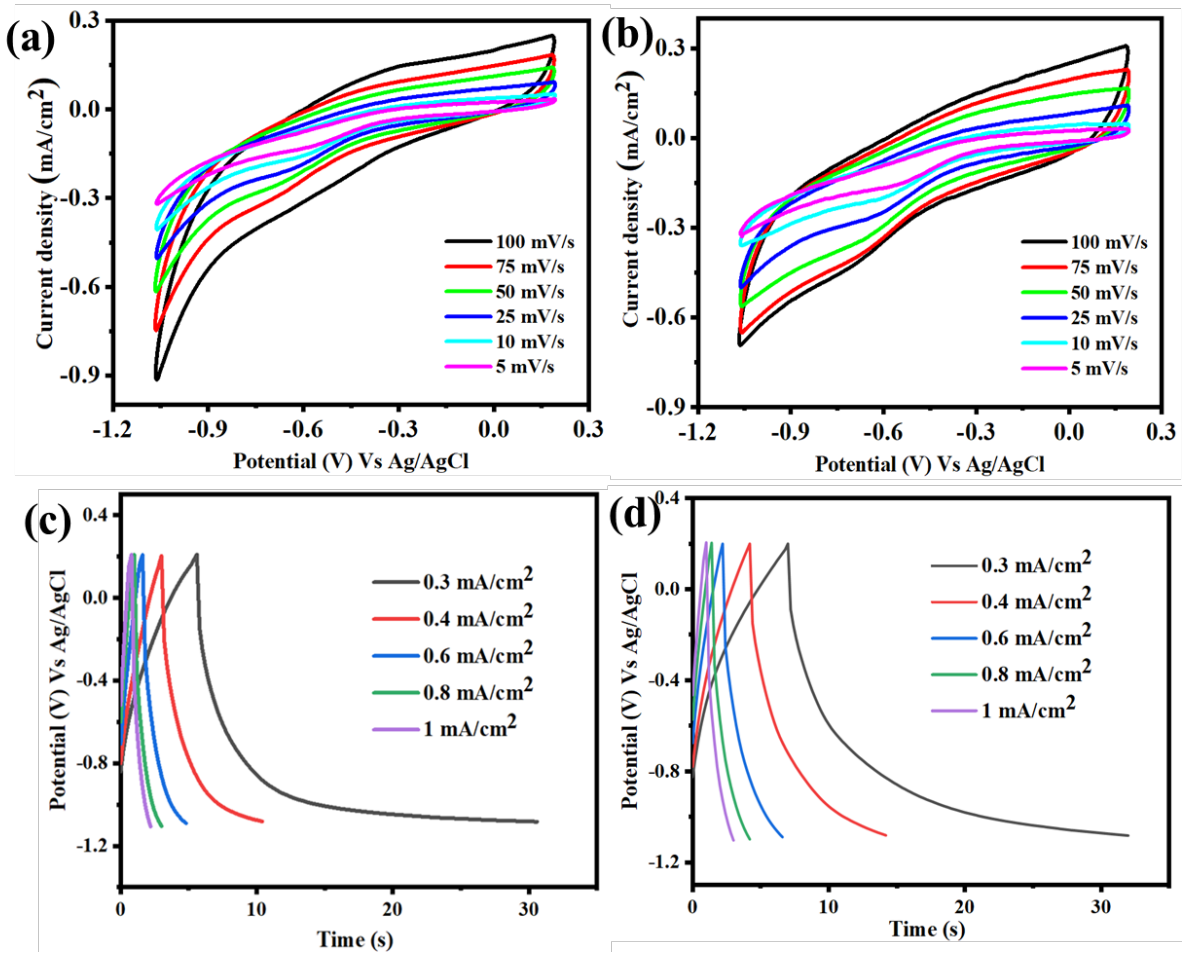

Figure S18. CV curves of electrodes **(a) V-SS-1** and **(b) V-SS-2** at varying scan rates from 5-100 mV/s, and GCD plots of electrodes **(c) V-SS-1** and **(d) V-SS-2** at varying current densities 0.3 to 1 mA/cm^2.

.

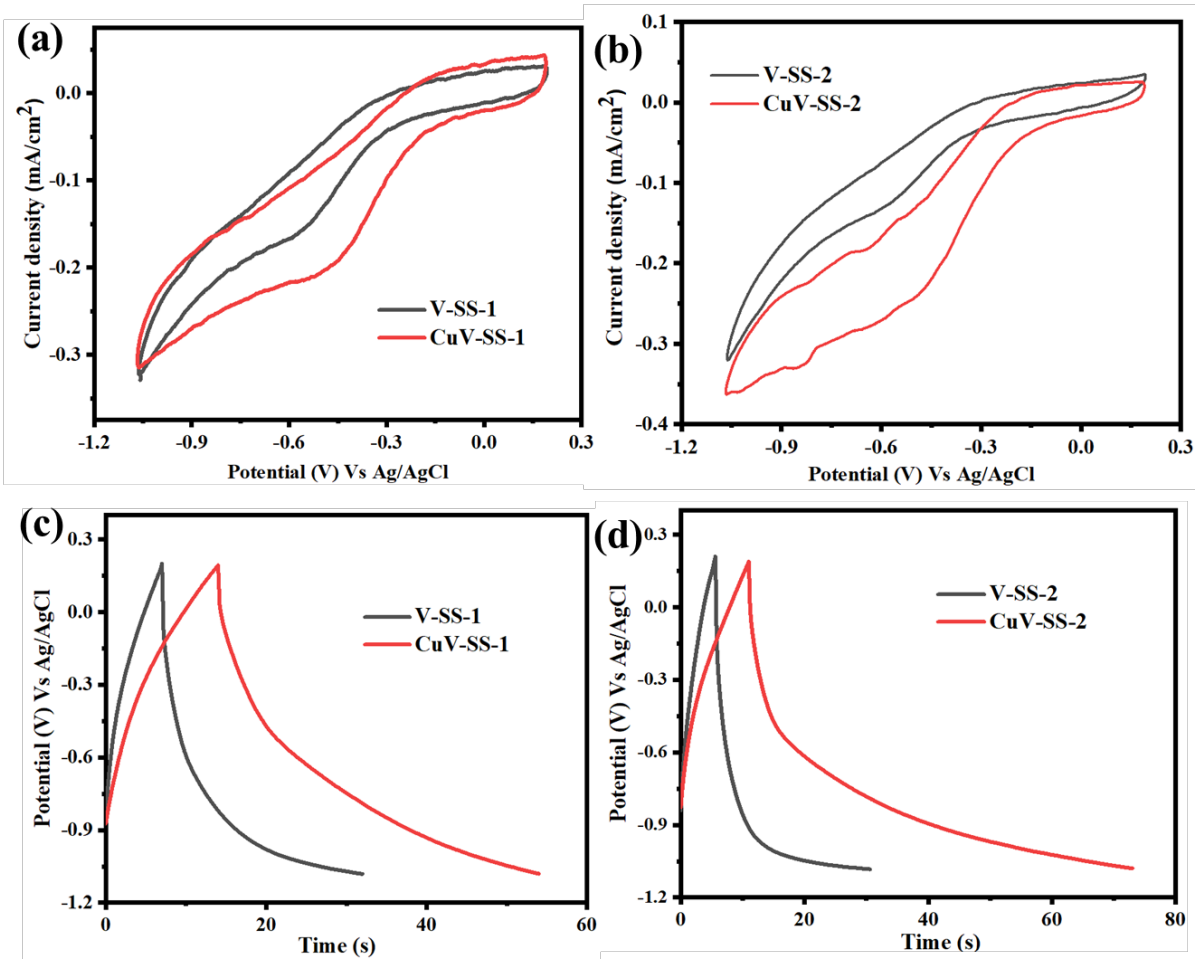

Figure S19. Comparative CV plots of **(a) V-SS-1** *vs* **CuV-SS-1**, **(b) V-SS-2** *vs* **CuV-SS-2, (c)** Comparative GCD curves of **(c) V-SS-1** *vs* **CuV-SS-1**, **(d) V-SS-2** *vs* **CuV-SS-2**.

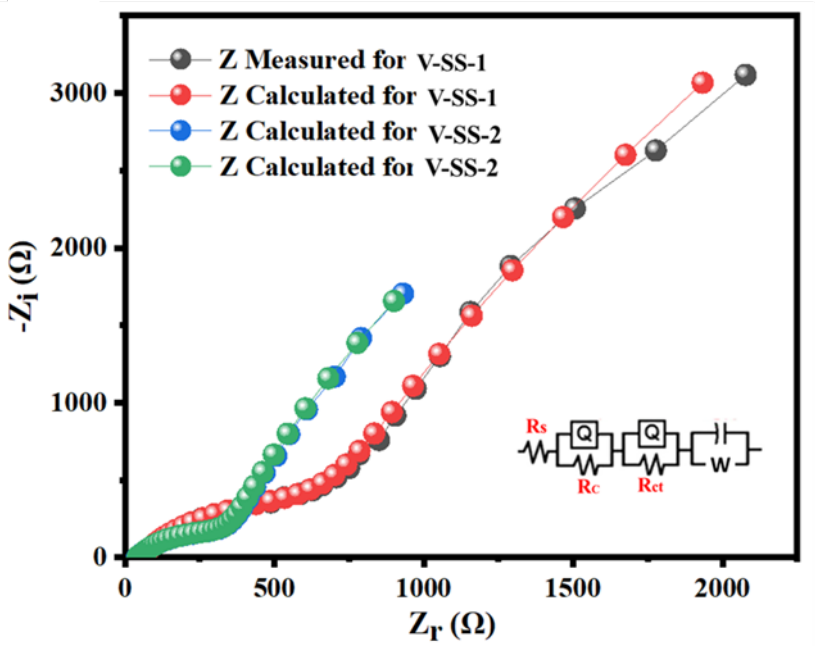

Figure S20. Nyquist plots of electrodes **V-SS-1** and **V-SS-2**. (inset shows fitiing circuit)

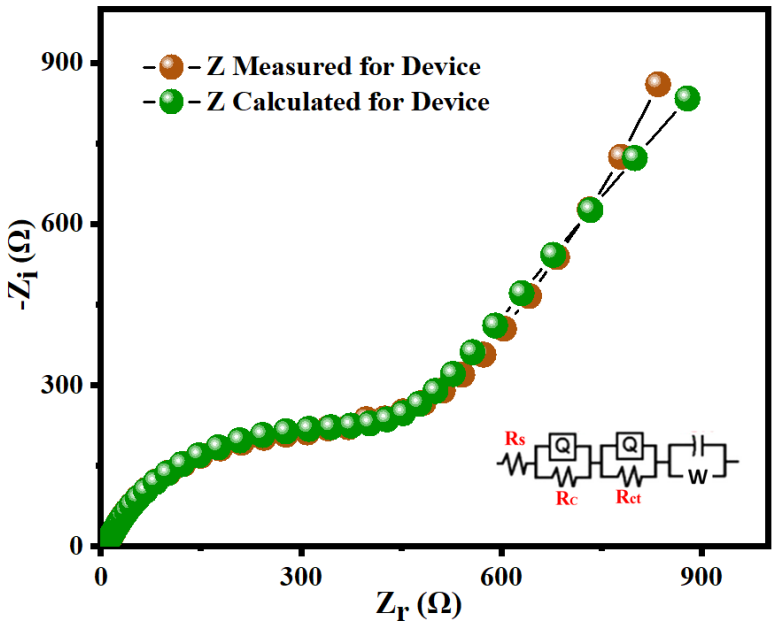

Figure S21: Nyquist plot of device.(inset shows fitting circuit)

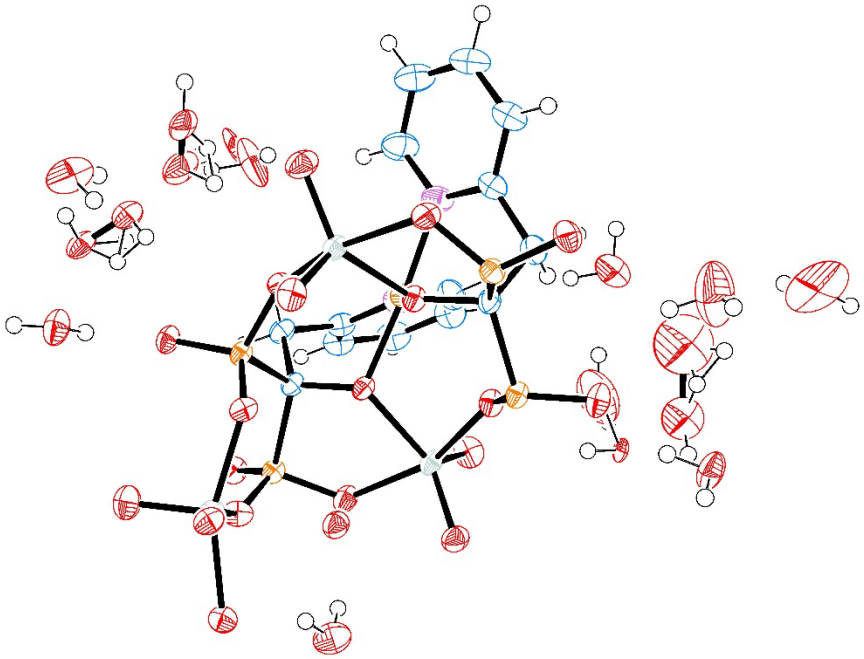

(a)

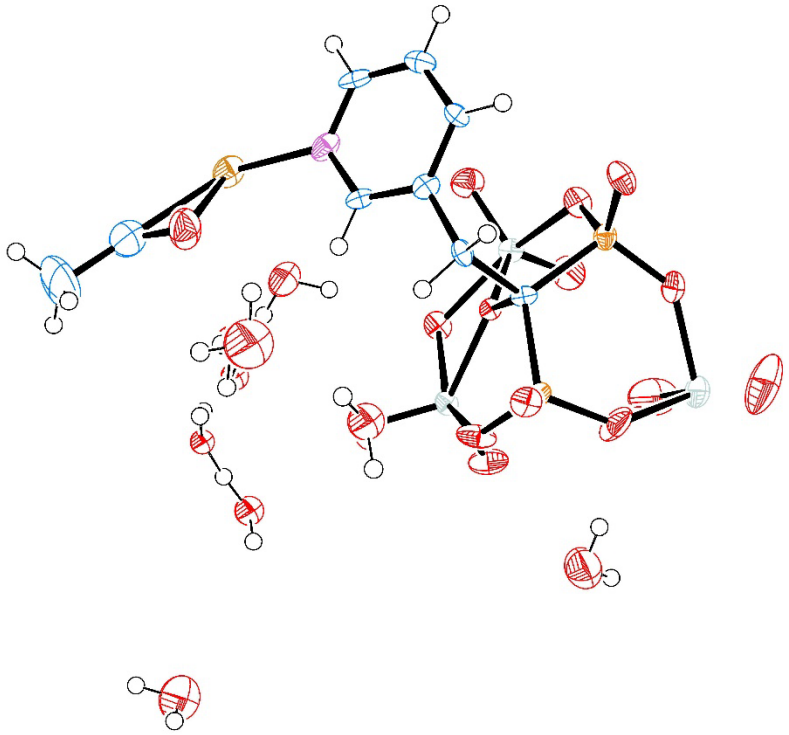

(b)

Figure S22. ORTEP representation of the asymmetric unit structures of **(a) CuV-1** and **(b) CuV-2**, at 50% thermal ellipsoid probability, showing ADPs. Color code: copper, yellow; vanadium, grey; nitrogen, purple; oxygen, red; carbon, blue; chlorine, yellow; sodium, green; hydrogen, white.